Dynamic Modeling and Integral Sliding Mode Controller Design for the Cuk Inverter*

ByeongCheol Han[1], Minsung Kim[2], Sungho Lee[3], and Jin S. Lee[1]
[1] Department of Creative IT Engineering, POSTECH, Republic of Korea.
[2] Future IT Research Laboratory, POSTECH, Republic of Korea.
[3] Department of Electrical Engineering, POSTECH, Republic of Korea.
77 Cheongam-Ro. Nam-Gu. 790-784
Pohang, Republic of Korea
Email: hbychol@postech.ac.kr

Keywords

Buck-boost converter, sliding mode control, DC-AC inverter, Cuk converter.

Abstract

This paper proposes a PWM based integral sliding mode controller (ISMC) for the single-stage Cuk inverter. The fourth-order model of the Cuk inverter is derived first and it is simplified to use ISMC. Based on the simplified system model, the ISMC that consists of the equivalent control part plus the switching control part is designed and applied to the single-stage Cuk inverter. Comparing to conventional controller, the ISMC can accurately control the output current of the single-stage Cuk inverter. Simulation and experimental tests using the prototype of the single-state Cuk inverter were performed to validate the proposed control approach.

Introduction

Cuk converters are mainly applied to the dc power supplies capable of operating in step-up and step-down mode. It uses the capacitor for energy transfer, while other converters such as buck and boost converters use the inductor to do it [1]. Moreover, the Cuk converter has continuous voltage and current at both input and output terminals, thereby keeping the number of components and the component size small [5]. Cuk converters are widely used in industries such as wind energy [2], photovoltaic power system [3],[5], electrical vehicle [4] and fuel cell charger [6].

Among the controllers used for converters, proportional-integral-derivative (PID) control technique is most popular due to its simplicity and robustness. However, designing a stable Cuk converter by using the PID controller is not easy. To guarantee stable operation with the PID controller, we must use large size capacitors to decouple input and output stages. They also need to support the full-load current, and so it becomes more expensive [5]. Furthermore, PID controller often fails to perform under large parameter and load variations [7].

To utilize a low-priced and small capacitors in the Cuk converter design and attain a good performance under parameter and load variations, a number of researchers have applied SMC to Cuk converters. One of the most popular SMC is the Hysteresis-Modulation (HM)-based SMC [11], which was designed based on a complex fourth-order model [8]. And it was developed under both complete state feedback and reduced state feedback settings [9]. In practice, the Cuk converter with HM based SMC was mainly used in solar inverter, and it used much smaller, more reliable nonelectrolytic capacitors [5]. Recently,

*This research was supported by the MSIP(Ministry of Science, ICT and Future Planning), Korea, under the "ICT Consilience Creative Program" (IITP-2015-R0346-15-1007) supervised by the IITP(Institute for Information & communications Technology Promotion).

the combined PI and SMC was proposed to regulate a fourth-order Cuk converter, and its PI gains are obtained by using the Routh-Hurwitz stability criterion and root locus [10].

However, the HM-based SMC generally suffers from significant switching-frequency variation when the input voltage and the output load are varied [11, 19, 20]. This variation complicates design of the input and output filters, because oversized filters may be required to cover a worst case frequency condition. The switching frequency variation also deteriorates regulation properties of the converters. Thus, it is necessary to design SMC for the Cuk converter that operates at a constant switching frequency even under input and output variations.

SMC that operates at constant switching frequency can be developed by employing pulse width modulation (PWM) instead of HM [12]. In practice, this is similar to classical PWM control schemes in which the control signal is compared to the ramp waveform to generate a discrete gate pulse signal. The advantage of this approach is that the additional circuits are not required since the switching function is performed by the PWM modulator, and so its transient response is not deteriorated. However, PWM based SMC can cause steady-state errors [21]. Moreover, the robustness property of the conventional SMC with respect to system parameter variations and external disturbances can only be achieved in the sliding mode phase. During the reaching phase, we cannot guarantee robustness [17].

The integral sliding mode controller (ISMC) was first introduced in [13]. ISMC aims at eliminating the reaching phase so that the system robustness is guaranteed from the initial stage. PWM based ISMC was developed for Buck converter in [23] and Boost converter in [21]. In these research works, the SMC based on PWM method consists of the equivalent controller only without any switching control function.

Cuk topology has been adopted to the single-stage inverter [5, 24, 25], and PI and Proportional-resonant (PR) control were used in [24, 25] and the cuk inverter for HM based SMC scheme was designed in [5]. In this paper, we propose the PWM based ISMC with a switching controller for the single-stage Cuk inverter. It uses both the equivalent controller and the switching controller which enable to employ a certain sliding surface as a reference path. Simplified dynamic model of the Cuk inverter is derived to use the ISMC, which can reduce the computation burden. Corresponding to the simplified, we developed ISMC for the Cuk inverter. We perform numerical simulations to test the proposed ISMC. Finally, we conducted experimental tests to demonstrate its practical feasibility.

Preliminary and Problem Formulation

Single-stage Cuk inverter

The single-stage Cuk inverter consists of the Cuk inverter with rectified sinusoidal output and the unfolding bridge (Fig. 1). The former is a high-frequency DC-DC stage which generates the rectified sinusoidal wave and the latter is low-frequency unfolding stage which creates the full wave of the sinusoid.

The modeling of Cuk inverter

The equivalent circuit of the Cuk inverter is presented in (Fig. 2). The Cuk inverter is constructed by combining a Boost converter and a Buck converter, and contains two inductor L_1, L_2, two capacitors C_1,

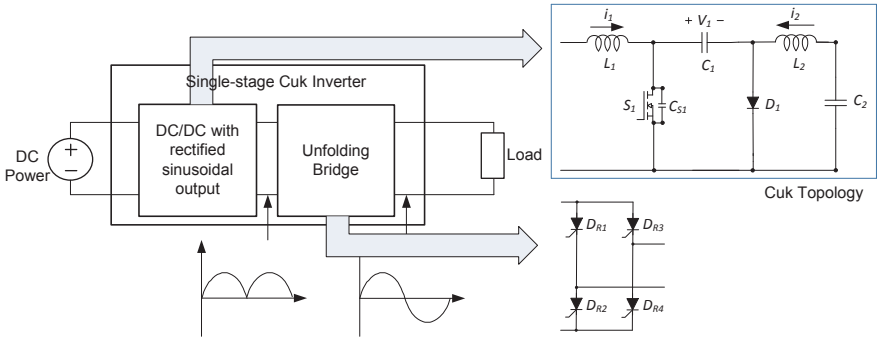

Figure 1: The circuit diagram of single-stage Cuk inverter.

C_2, and load resistance R_L. The operation principle of Cuk converter can be described as follows. When the switch S_1 is closed, the current flowing through the inductor L_1 increases. Diode D_1 is counterpolarized, and the capacitor C_1 supplies the energy to the output stage. The current that flows through the inductor L_2 also increases while the voltage across the capacitor C_1 decreases. When the switch S_1 is open, both inductor currents that flow through the free-wheeling diode D_1 decrease, and capacitor C_1 set recharged with current i_1.

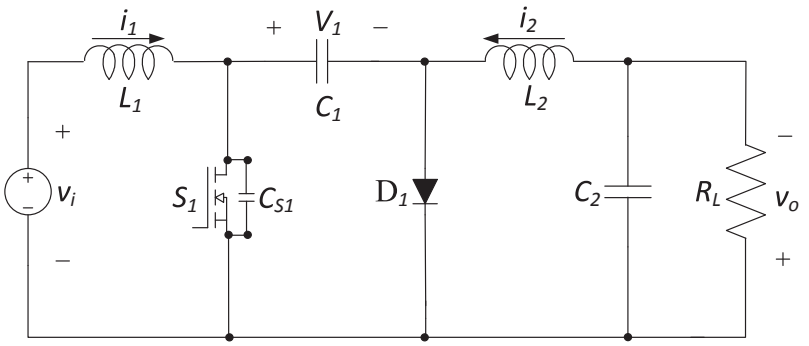

Figure 2: The equivalent circuit of Cuk inverter.

The state-space equations in the turn-on and turn-off subintervals are expressed in the following equations, respectively:

$$L_1\frac{di_1(t)}{dt} = v_i(t), \tag{1}$$

$$L_2\frac{di_2(t)}{dt} = v_1(t) - v_o(t), \tag{2}$$

$$C_1\frac{dv_1(t)}{dt} = -i_2(t), \tag{3}$$

$$C_2\frac{dv_o(t)}{dt} = i_2(t) - \frac{v_o(t)}{R_L}, \tag{4}$$

and

$$L_1\frac{di_1(t)}{dt} = v_i(t) - v_1(t), \tag{5}$$

$$L_2\frac{di_2(t)}{dt} = -v_o(t), \tag{6}$$

$$C_1\frac{dv_1(t)}{dt} = i_1(t), \tag{7}$$

$$C_2\frac{dv_o(t)}{dt} = i_2(t) - \frac{v_o(t)}{R_L}. \tag{8}$$

where $i_1(t)$ is the current that flows through the input inductor L_1, $i_2(t)$ is the current that flows through the output inductor L_2, $v_1(t)$ is the voltage across the transfer capacitor C_1, and $v_o(t)$ is voltage across the output capacitor C_2. $v_i(t)$ and $v_o(t)$ respectively represent the input and output voltages, and R_L represents the resistive load.

Combining (1)–(4) and (5)–(8) using the state-space averaging method, the averaged model equations can be described as

$$\frac{di_1(t)}{dt} = \frac{1}{L_1}v_i(t) - \frac{1}{L_1}(1-D)v_1(t), \tag{9}$$

$$\frac{di_2(t)}{dt} = \frac{1}{L_2}Dv_1(t) - \frac{1}{L_2}v_o(t), \tag{10}$$

$$\frac{dv_1(t)}{dt} = -\frac{1}{C_1}Di_2(t) + \frac{1}{C_1}(1-D)i_1(t), \tag{11}$$

$$\frac{dv_o(t)}{dt} = \frac{1}{C_2} i_2(t) - \frac{1}{R_L C_2} v_o(t), \tag{12}$$

where D is the control duty ratio.

Control scheme

Simplified dynamic equation for output voltage control

The above dynamic equations (9)–(12) can be used to construct the sliding mode controllers. But the direct use of the above dynamic equations for controller design is too complex, because the four-dimension matrix needs to be solved, and the four parameters need to be measured. Instead, we suggest to use the following simplified dynamic equations for output voltage control of the Cuk converter. Taking the time derivative on both sides of (12) and substituting both (10) and (12) into the this derivative equation, we have

$$\frac{dx_1(t)}{dt} = x_2(t), \tag{13}$$

$$\frac{dx_2(t)}{dt} = f(x_1(t), z_1(t)) + g(z_2(t))u(t) + v(t), \tag{14}$$

$$y_1(t) = x_1(t), \tag{15}$$

where $\mathbf{x}(t) = [x_1(t), x_2(t)] = [v_o(t), \frac{1}{C_2} i_2(t) - \frac{1}{R_L C_2} v_o(t)]$, $z_1(t) = i_2(t)$, $z_2(t) = v_1(t)$ are the state, $y_1(t)$ is the output, $u(t) = D$ is the control input, $f(x_1(t), z_1(t))$ and $g(z_2(t))$ are the system function and the control gain, and $v(t)$ is a lumped uncertainty; $f(x_1(t), z_1(t))$ and $g(z_2(t))$ are represented as

$$f(x_1(t), z_1(t)) = \left(-\frac{1}{L_2 C_2} + \frac{1}{(R_L C_2)^2} \right) x_1(t) - \frac{1}{R_L C_2^2} z_1(t), \tag{16}$$

$$g(z_2(t)) = \frac{1}{L_2 C_2} z_2(t), \tag{17}$$

and

$$v(t) = \Delta v(x_1(t), z_1(t), z_2(t), d(t)), \tag{18}$$

where $d(t)$ is the unknown external disturbance. This uncertainty satisfies the matching condition

$$v(t) \in \text{span}(g(z_2(t))). \tag{19}$$

The objective of the controller is to drive the output voltage of the Cuk inverter to follow a reference output voltage in the presence of uncertain parameters and unknown disturbances. The lumped uncertainty $v(t)$ may deteriorate the control performance and even cause the system to go unstable. To overcome the problem, we propose an integral sliding mode controller (ISMC) for the Cuk inverter in the following section. The aim of the ISMC is to constrain the output voltage of the Cuk inverter to stay on a sliding surface $s(t) = 0$, and thereby keeping the error variables stay on the prescribed error dynamics.

Integral sliding mode controller design for the Cuk inverter

To help better understand the integral sliding mode controller, we start with choosing the sliding manifold of the conventional sliding mode controller, which is well known for its robustness to parameter uncertainties and external disturbances [18]. The conventional sliding surface is defined as $s(t)$ where

$$s(t) = \left(\lambda + \frac{d}{dt} \right)^{n-1} e_1(t), \tag{20}$$

where n denotes the system order, $e_1(t) = y_{1d}(t) - y_1(t)$ represents the tracking error, λ is a positive constant; $y_{1d}(t)$ is the reference output voltage.

In addition to the robustness property against the parameter uncertainties and disturbances, the ISMC improves the steady-state accuracy by including the integral action to the conventional sliding surface. The integral augmented sliding surface is given as [13]:

$$s(t) = (\lambda + \frac{d}{dt})^{n-1} e_1(t) + k_i \int_0^t e_1(\tau) d\tau - \left(\lambda + \frac{d}{dt}\right)^{n-1} e_1(0), \tag{21}$$

where k_i is a positive constant.

We now set the system order $n = 2$ and take the derivative of the integral augmented sliding surface $s(t)$ with respect to time:

$$\dot{s}(t) = \ddot{e}_1(t) + \lambda \dot{e}_1(t) + k_i e_1(t). \tag{22}$$

Substituting (13) and (14) into (22) yields

$$\dot{s}(t) = \ddot{y}_{1d}(t) - f(x_1(t), z_1(t)) - g(z_2(t))u(t) + v(t) + \lambda \dot{e}_1(t) + k_i e_1(t). \tag{23}$$

By setting $\dot{s}(t) = 0$, the equivalent control law can be obtained as

$$u_{eq}(t) = g^{-1}(z_2(t))(\ddot{y}_{1d}(t) + \lambda \dot{e}_1(t) + k_i e_1(t) - f(x_1(t), z_1(t))), \tag{24}$$

where λ and k_i are selected such that the polynomial $\ddot{e}_1(t) + \lambda \dot{e}_1(t) + k_i e_1(t)$ becomes Hurwitz. Applying the control law (24) into (23) yields the resulting error dynamics

$$\begin{aligned} \dot{s}(t) &= \ddot{e}_1(t) + \lambda \dot{e}_1(t) + k_i e_1(t) \\ &= v(t), \quad |v(t)| < \bar{v} \end{aligned} \tag{25}$$

where $\bar{v}$ is the upper bound of the bias term. If the bias term $v(t)$ is zero, then we obtain the ideal error dynamics

$$\dot{s}(t) = \ddot{e}_1(t) + \lambda \dot{e}_1(t) + k_i e_1(t) = 0. \tag{26}$$

However, the bias term $v(t)$ prevents the tracking error $e_1(t)$ from converging to zero. To suppress this bias term, we choose to use the switching control input as [18]:

$$u_{sw}(t) = g^{-1}(z_2(t)) k_{sw} sgn(s(t)), \tag{27}$$

where k_{sw} is a positive constant, $k_{sw} \geq \bar{v} + \eta$ where η is a positive constant, and the signum fuction $sgn(\cdot)$ is defined as

$$sgn(x) = \begin{cases} -1, & \text{if } x < 0 \\ 0, & \text{if } x = 0 \\ 1, & \text{if } x > 0. \end{cases} \tag{28}$$

Combining the equivalent and switching control laws, we have the complete control law as:

$$\begin{aligned} u(t) &= u_{eq}(t) + u_{sw}(t) \\ &= g^{-1}(z_2(t))(\ddot{y}_{1d}(t) + \lambda \dot{e}_1(t) + k_i e_1(t) - f(x_1(t), z_1(t))) + g^{-1}(z_2(t)) k_{sw} sgn(s(t)). \end{aligned} \tag{29}$$

This control scheme (Fig. 2) consists of three elements. The feedback term $g(z_2(t))^{-1}(-\lambda \dot{e}_1(t) - k_i e_1(t))$ makes the closed-loop system stable within a uniform error bound; the term -$g(z_2(t))^{-1}(f(x_1(t), z_1(t)))$ cancels system nonlinearity; the switching input $-g(z_2(t))^{-1} k_{sw} sgn(s(t))$ suppresses the bias term $v(t)$.

Remark 1. Discontinuous switching control usually results in chattering that may excite undesirable high frequencies or unmodeled dynamics. The chattering phenomenon can be suppressed by using smoothing approximation of a sign function. A saturation function can serve as an example that can replace a sign function with [13]:

$$\text{sgn}(s(t)) \rightarrow \text{sat}(s(t)/\phi), \tag{30}$$

where $\phi > 0$ represents the thickness of the boundary layer, which should be adjusted to achieve an optimal balance of tracking performance and chattering reduction. Then, the resulting control law can be written as

$$u^*(t) = g^{-1}(z_2(t))(\ddot{y}_{1d}(t) + \lambda \dot{e}_1(t) + k_i e_1(t) - f(x_1(t), z_1(t))) + g^{-1}(z_2(t)) k_{sw} \text{sat}(s(t)/\phi). \tag{31}$$

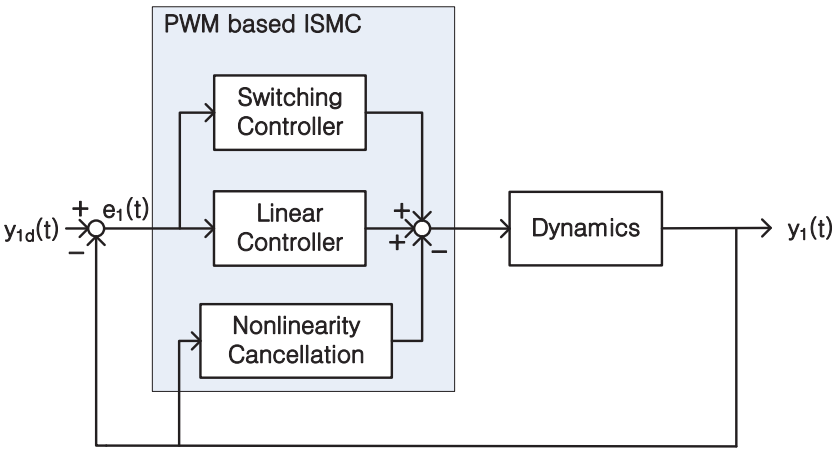

Figure 3: The schematic diagram of control system for the Cuk inverter.

Simulation Results

To test the feasibility of the developed controller, various computer simulations are conducted with a Cuk inverter model. The dynamics of the Cuk inverter are given as

$$\frac{dx_1(t)}{dt} = x_2(t), \tag{32}$$

$$\frac{dx_2(t)}{dt} = \left(-\frac{1}{L_2C_2} + \frac{1}{(R_LC_2)^2}\right)x_1(t) - \frac{1}{R_LC_2^2}z_1(t) + \frac{1}{L_2C_2}z_2(t)u(t) + \Delta v(x_1(t), z_1(t), z_2(t), d(t)), \tag{33}$$

$$y_1(t) = x_1(t), \tag{34}$$

where we set the input voltage $V_i = 50\ V$, the desired peak sinusoidal output voltage $V_{do} = 220\ V_{rms}$, the output frequency $f_0 = 60Hz$, the capacitance $C_1 = 200\ nF$, $C_2 = 500\ nF$, the inductance $L_1 = 200\ uF$, $L_2 = 400\ uF$, and the switching frequency $f_s = 50\ kHz$. The control input is selected as

$$u^*(t) = g^{-1}(z_2(t))(\ddot{y}_{1d} + \lambda\dot{e}_1(t) + k_i e_1(t) - f(x_1(t), z_1(t))) + g^{-1}(z_2(t))k_{sw}\text{sat}(s(t)/\phi), \tag{35}$$

where we set $\lambda = 2 \times 10^7$, $k_i = 4 \times 10^4$, $k_{sw} = 4.6 \times 10^4$, ϕ = 0.1. We simulate this example with the PSIM software. Under the above setting and the input command $v_{do} = 220\ V_{rms}$, we tested the equivalent controller (PD controller plus nonlinear cancellation) and the proposed ISMC.

When the equivalent control input is used, the waveforms of output voltage is distorted (Fig. 4(a)). When ISMC is used, the trajectories of the output voltage track the desired output voltage more accurately (Fig. 5(a)). To demonstrate the performance of the proposed controller, we examined the rms errors of the output voltage in Fig. 5(b), 5(b). The rms error with the proposed controller is generally smaller than that with the equivalent controller. We also examined the root-mean-square (RMS) error and total harmonic distortion (THD) of the output voltage in Fig. 6(a), 6(b). The RMS error and THD with the proposed ISMC are smaller than those with the equivalent controller within all input voltage range. controller has better output tracking ability.

Experiment

To demonstrate practical feasibility of the developed controller, the proposed control algorithm was applied to an experimental prototype of the Cuk inverter. The controller was developed utilizing the MPC5554EVB reference board. We set the input command ($V_{do} = 110\ V_{rms}$) and control parameters as $\lambda = 1.3 \times 10^7$, $k_i = 9 \times 10^4$, and $k_{sw} = 1.8 \times 10^4$. The main components and parameters of the prototype used for experiments were shown in Table I.
We tested the single-stage Cuk inverter equipped with the equivalent controller and that with plus the switching controller. When the equivalent controller is used, the output tracking performance was poor

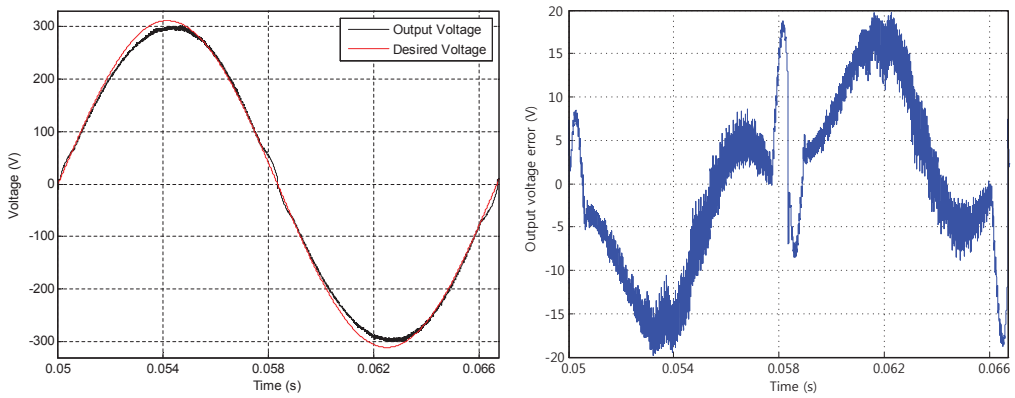

(a) (b)

Figure 4: Simulation results with the equivalent controller under the input voltage is 50 V. (a) Output voltage waveform. (b) Output voltage error.

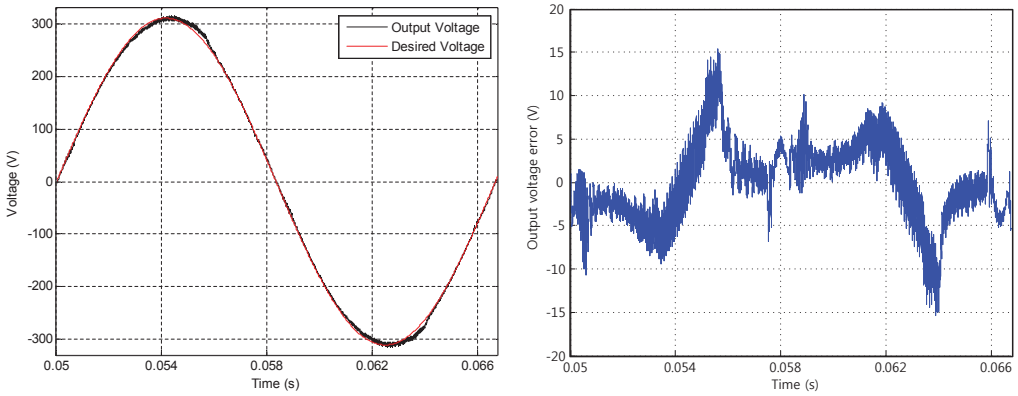

(a) (b)

Figure 5: Simulation results with the proposed ISMC when the input voltage is 50 V. (a) Output voltage waveform. (b) Output voltage error.

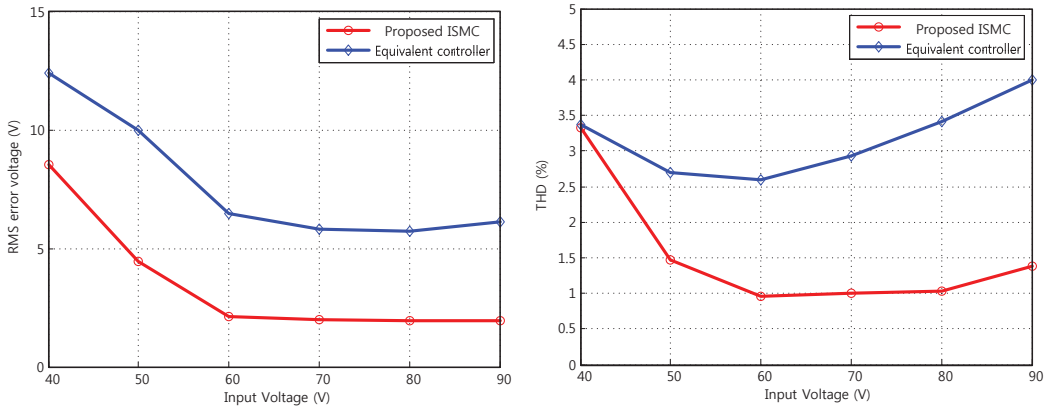

(a) (b)

Figure 6: Simulation results as the input voltage varies from 40 V to 90 V. (a) RMS of output voltage error. (b) THD.

near zero crossing region. At the peak, the output voltage with the equivalent controller was about 148 V which is much less than the desired voltage (Fig. 7(a)). When the proposed ISMC was used, the switching control input suppressed the disturbance, thereby eliminating the steady-state error near zero voltage. At the peak, the output voltage tracks well the desired output voltage (Fig. 7(b)).

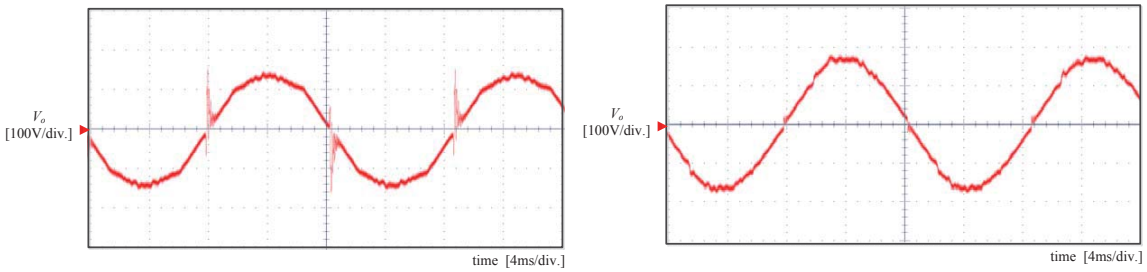

(a) (b)

Figure 7: Experimental waveforms of output voltage. (a) When the equivalent controller is used. (b) When the proposed ISMC is used.

Table I: Parameters and components of the prototype Cuk converter

Parameters	**Symbols**	**Value**
Input voltage	V_i	50 V
Desired output voltage	V_{do}	110 V_{rms}
Desired output frequency	f_{do}	60 Hz
Switching frequency	f_s	50 kHz
First capacitance	C_1	200 nF
Second capacitance	C_2	500 nF
First inductance	L_1	200 μF
Second inductance	L_2	400 μF
Components	**Symbols**	**Part number**
Switch	S_1	HGTG30N60A4D
Gate Driver	G_1	SKHI 22B R
Diode	D_1	E20U60DN
Switch	$D_{R1}, D_{R2}, D_{R3}, D_{R4}$	SPA11N60C3

Conclusion

This paper presented a fixed-frequency PWM based integral sliding mode control design for the single-stage Cuk inverter. The model of the Cuk inverter is derived and simplified to use the ISMC without complex computation. The ISMC is designed and applied to the single-stage Cuk inverter. We compared the performances of the PD controller plus nonlinear cancellation term and the proposed ISMC by using the simulation and experimental results and verified that the proposed controller is superior in tracking accuracy.

References

[1] B. K. Kushwaga and A. Narain : Controller Design for Cuk Converter Using Model Order Reduction, International Conference on Power, Control and Embedded Systems (ICPCES), PP. 1-5, 2012.

[2] G. Su, W. Gong, L. Pan, R. Gao, and B.B. Wang : Maximum power point tracking of photovoltaic, Chines Control Conference (CCC), pp. 4880-4884, Jul. 2010.

[3] H. Chung, K. Tse, S. Hui, C.M.Mok, and M.T.Ho : A novel maximum power point tracking technique for solar panels using a SEPIC or Cuk converter", IEEE Transactions on Power Electronics, Vol. 18, no. 3, pp. 717-724, May 2003.

[4] Y. Fan, L. M. Ge, and W. Hua : Multiple-input DCDC converter for the thermoelectric-photovoltaic energy system in hybrid electric vehicles, IEEE Vehicle Power Propulsion Conference, pp. 35-40, Aug. 2010.

[5] J. Knight, S. Shirsavar and W. Holderbaum : An Improved Reliability Cuk Based Solar Inverter With Sliding Mode Control, IEEE Transactions on Power Electronics, vol. 21, no. 4, pp. 1107-1115, Jul. 2006.

[6] T. H. Kim, N. V. Sang, and W. Choi : Control of The Portable Fuel cell charger using Cuk converter, IEEE Transactions on Power Electronics, vol. 2, no. 5, pp. 1655-1667, May 2013.

[7] V. S. C. Raviraj and P. C. Sen : Comparative study of proportional-integral, sliding mode, and fuzzy logic controllers for power converters, IEEE Transactions on Industry Applications, vol. 33 no. 2, pp. 518-524, Mar./Apr. 1997.

[8] S. P. Huang, H. Q. Xu, and Y. F. Liu : Sliding-mode controlled Cuk switching regulator with fast response and first-order dynamic chacteristic, Annual IEEE Power Electronics Specialists Conference, pp. 124-129, Jun. 1989.
[9] L. Malesani, L. Rossetto, G. Spiazzi, and P. Tenti : Performance Optimization of Cuk Converters by Sliding Mode Control, IEEE Transactions on Power Electronics, vol. 10, no. 3, pp. 302-309, May 1995.
[10] Z. Chen : PI and Sliding Mode Control of a Cuk Converter, IEEE Transactions on Power Electronics, vol. 27, no. 8, pp. 3695-3703, Aug. 2012.
[11] S. Tan, Y. M. Lai, and C. K. Tse : General Design Issues of Sliding-Mode Controllers in DC-DC Converters, IEEE Transactions on Industry Electronics, vol. 55, no. 3, pp. 1160-1174, Mar. 2008.
[12] V. M. Nguyen and C. Q. Lee : Indirect implementations of sliding-mode control law in buck-type converters, IEEE Applied Power Electronics Conference, Vol. 1, pp. 111-115, Mar. 1996.
[13] V. Utkin and J. Shi : Integral Sliding Mode Control in Systems Operating under Uncertainty Conditions, IEEE Conference On Decision and Control (CDC), pp. 4591-4596, Dec. 1996.
[14] R. K. Lea, R. Allen and S. L. Merry : A comparative study of control techniques for an underwater flight vehicle, International Journal of Systems Science, vol. 30, no. 9, pp. 947-964, 1999.
[15] M. Fu, X. Bian, W. Wang and J. Gu : Research on sliding mode controller with an integral applied to the motion of underwater vehicle, IEEE International Conference on Mechatronics and Automation, vol. 4, pp. 2144-2149, 29 Jul.-1 Aug. 2005.
[16] Z. Tang, J. Zhou, X. Bian and H. Jia : Simulation of optimal integral sliding mode controller for the depth control of AUV, IEEE International Conference on Information and Automation (ICIA), pp. 2379-2383, Jun. 2010.
[17] J. Shi, H. Liu and N. Bajcinca : Robust control of robotic manipulators based on integral sliding mode, International Journal of Control, vol. 81, no. 10, pp. 1537-1548, Oct. 2008.
[18] J. J. Slotine, and W. Li : Applied nonlinear control, New Jersey: Prentice hall 1991.
[19] P. Mattavelli, L. Rossetto, G. Spiazzi, and P. Tenti : General-purpose sliding-mode controller for DC/DC converter applications, IEEE Annual Power Electronics Specialists Conference, pp. 609-615, Jun. 1993.
[20] S. C. Tan, Y. M. Lai, M. K. H. Cheung, and C. K. Tse : On the practical design of a sliding mode voltage controlled buck converter, IEEE Transactions on Power Electronics, vol. 20, no. 2, pp. 425-437, Mar. 2005.
[21] S. C. Tan, Y. M. Lai, C. K. Tse, and C. K. Wu : A Pulsewidth Modulation Based Integral Sliding Mode Current Controller for Boost Converters, IEEE Annual Power Electronics Specialists Conference, pp. 1-7, Jun. 2006.
[22] H. K. Khalil : Nonlinear systems, vol. 3, Upper Saddle River: Prentice HALL 2002.
[23] S. C. Tan, Y. M. Lai, C. K. Tse, and M. K. H. Cheung : A Fixed-Frequency Pulsewidth Modulation Based Quasi-Sliding-Mode Controller for Buck Converters, IEEE Transactions on Power Electronics, vol. 20, no. 6, pp. 1379-1392, Nov. 2005.
[24] S. Mehrnami and Sudip K. Mazumder : Discontinous Modulation Scheme for a Differential-Mode Cuk Inverter, IEEE Transactions on Power Electronics, vol. 30, no. 3, pp. 1242-1254, Mar. 2015.
[25] A. Darwish, D. Holliday, S. Ahmed, A. M. Massoud, and B. W. Williams : A Single-Stage Three-Phase Inverter Based on Cuk Converters for PV Applications, IEEE Journal of Emerging and Selected Topics in Power Electronics, vol. 2, no. 4, pp. 797-807, Dec. 2014.